ELSEVIER

Thin Solid Films 326 (1998) 83–87

thin solid films

Nozzle diameter effects on $CuInSe_2$ films grown by ionized cluster beam deposition

Kenichi Kondo[a,*], Hiroyuki Sano[a], Katsuaki Sato[b]

[a]*Tsukuba Research Laboratory, Stanley Electric Co., Ltd., 5-9-5 Tokodai, Tsukuba, Ibaraki 300-26, Japan*
[b]*Faculty of Technology, Tokyo University of Agriculture and Technology, 2-24-16 Nakacho, Koganei, Tokyo 184, Japan*

Received 25 November 1997; accepted 13 February 1998

Abstract

Thin films of the chalcopyrite semiconductor $CuInSe_2$ were grown by an ionized cluster beam (ICB) deposition technique at a low substrate temperature of 300°C. We studied the effect of nozzle diameter (a perforation on the top lid of the crucibles) of the cluster-source crucibles on the thin films. The diameters were 1.7, 2.0, or 3.0 mm. The deposited films obtained were characterized using scanning electron microscopy (SEM), X-ray diffraction (XRD), electron probe microanalysis (EPMA), scanning ion mass spectroscopy (SIMS), and Raman spectroscopy. Change in the nozzle diameter significantly affected both the intensity of the Raman peaks at 183 and 260 cm^{-1} and the crystallinity of the $CuInSe_2$ films. The maximum diameter for obtaining good crystallinity of $CuInSe_2$ films is between 2.0 and 3.0 mm. It is found that the energy of Cu clusters plays a very important role in the crystal growth of $CuInSe_2$.

Keywords: Cluster; Raman scattering; Solar cells; Crystallization

1. Introduction

The chalcopyrite semiconductor $CuInSe_2$ is a promising material for polycrystalline thin film solar cells because of its large absorption coefficient [1] and good radiation resistance [2,3]. Various fabrication methods, such as selenization method and co-evaporation, successfully achieve high conversion efficiency [4,5].

For low-cost thin film solar cells, we have been using ionized cluster beam (ICB) deposition to obtain $CuInSe_2$ and $CuGaSe_2$ films at low temperature. Although the effect of acceleration voltage [6–9], ionization current [10,11] and ionization of the Se source on the quality of the films [9] have been studied, no studies have been done on the effect of the nozzle diameter for cluster beams.

In the present study, we prepared $CuInSe_2$ thin films at low substrate temperature (300°C) using ICB with various nozzle diameters of the Cu source crucible (1.7, 2.0, and 3.0 mm). We then characterized these films using X-ray diffraction (XRD), scanning electron microscope (SEM), electron prove microanalysis (EPMA), secondary ion mass spectroscopy (SIMS), and Raman spectroscopy. In this paper, we report the results of this characterization and discuss the effect of ionized cluster beam on the crystallinity of $CuInSe_2$.

2. Experimental

An ICB technique was used to grow $CuInSe_2$ thin films on soda-lime glass substrates using the apparatus illustrated in Fig. 1. In this system, vapors of the individual source materials are ejected through the nozzle (a perforation on the top lid) of the crucible, subjected to adiabatic cooling, and then loosely united to form cluster beams. The clusters are then positively ionized by the bombardment of electrons emitted from the tungsten filament and extracted by a positive potential applied to the grid. The ionization current is defined as the current flowing between the filament and

* Corresponding author. E-mail: kenichi@stanley.trc-net.co.jp

0300-9440/98/$19.00
PII S0040-6090(98)00526-4

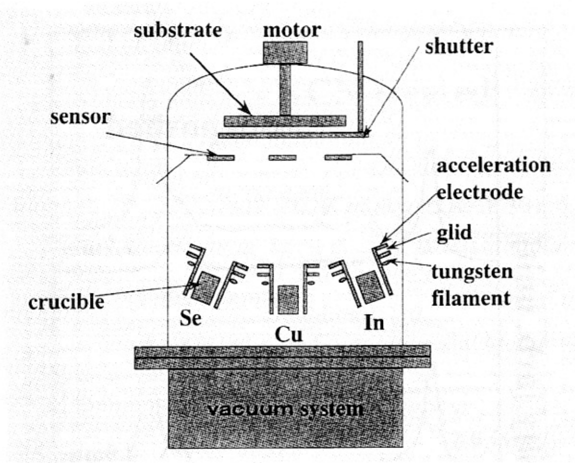

Fig. 1. Schematic of an ionized cluster beam deposition.

the grid. The ionized cluster beams are accelerated by a negative potential applied to an acceleration electrode set a few millimeters above the ionization system. In our experiments, both the Cu and In cluster beams were individually ionized and then accelerated. For the Cu source crucible (Fig. 2), the nozzle length L was 1 mm, and the nozzle diameter D was either 1.7, 2.0, or 3.0 mm. For the In and Se source crucibles, L = 1 mm and D = 1.5 mm. These dimensions for L and D satisfy the condition $L/D \leq 1$ determined by Yamada et al. [12] for the formation of clusters. Yamada et al. also reported that for successful cluster formation, the ratio of the pressure inside the crucible to the pressure outside the crucible must be larger than 10^4. During film deposition, the pressure of the vacuum chamber was maintained at less than 1×10^{-5} Torr. The temperatures of the crucibles for Cu, In, and Se were about 1420, 920, and 310°C, respectively. Because the vapor pressure of the Cu crucible exceeded 10^{-1} Torr, the above requirement was satisfied. The acceleration voltage for Cu and In was set at 1.5 KV and the ionization currents of Cu and In were 150 and 50 mA, respectively. The deposition rates of Cu, In, and Se were 0.1, 0.2, and 0.4 nm/s, respectively, and were monitored individually by crystal oscillators. The substrate temperature was kept at 300°C. The typical thickness of the prepared films was about 2 μm. Cyanide treatment is commonly used to remove binary phase of Cu–Se that generally exists on the surface of $CuInSe_2$ film that are Cu-rich, which is necessary to grow large grain $CuInSe_2$. We therefore etched the films using 10% KCN solution for 60 s and then rinsed them in deionized water. In the characterization of the films, XRD with Cu K_α was used for structural analysis, SEM for surface observation, EPMA for compositional determination, SIMS for depth profile of the components and Raman spectroscopy for structural analysis. In particular, to know the surface structure, Raman scattering experiments were done using a back-scattering configuration. The incident light of the Ar^+ laser (514.5 nm, 30 mW) was focused to about 1 mm diameter on a surface and the scattered beam was dispersed by a triple monochromator combined with a CCD photon counting apparatus. The polarized Raman spectra of horizontal–horizontal (HH) and horizontal–vertical (HV) configurations were done using a $\lambda/2$ plate and a polarizer. All measurements were taken at room temperature in air.

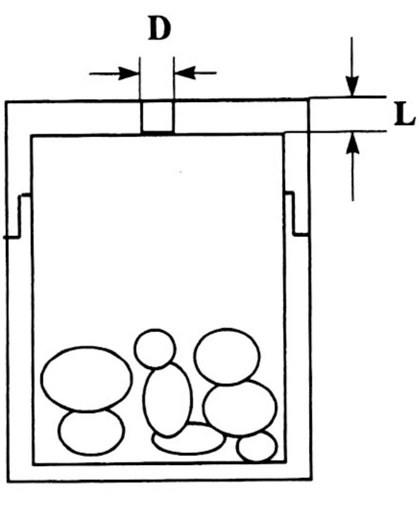

Fig. 2. Schematic of a crucible.

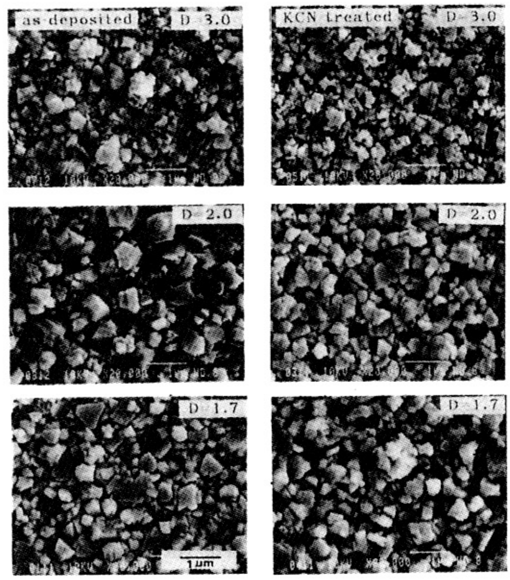

Fig. 3. SEM micrographs of the as-deposited and the KCN-treated films.

3. Results and discussion

SEM micrographs of as-deposited and KCN-treated $CuInSe_2$ films (Fig. 3) revealed that surface morphology and grain size strongly depended on *D*. There was a distinct difference in crystal size and surface morphology (Fig. 3) between the films of $D = 3.0$ and 2.0 mm. Among the $D = 3.0$, 2.0 and 1.7 mm, the size of the crystal grains of $D = 3.0$ mm was the smallest. The as-deposited Cu/In ratios measured by EPMA for all samples were in the 1.40–1.45 range. The XRD pattern for the as-deposited film of $D = 3.0$ (Fig. 4 is a typical pattern) show that the films contained Cu_3Se_2 (JCPDS: 190402) phase. All three films had similar XRD patterns, regardless of *D*. To obtain more information about the surface structures, we measured Raman spectra. The Raman spectrum for each film (Fig. 5) shows five peaks: 173, 183, 210, 230, and 260 cm^{-1}. The peak at 173 cm^{-1} is associated with the A_1 mode of $CuInSe_2$, 210 cm^{-1}, with either the E or B_2 mode, and 230 cm^{-1} with the E or B_2 mode [13,14]. The intensity of the peaks at 260 and 183 cm^{-1} decreased as *D* as decreased. The change in Raman spectrum was particularly drastic between the film of $D = 2.0$ and 3.0 mm.

The XRD patterns for the KCN-treated films were those of the single-phase chalcopyrite structure without any traces of the Cu_3Se_2 phase. Fig. 6 shows Raman spectra in the KCN-treated films. For all of the films, regardless of *D*, the intensity of the peak at 260 cm^{-1} was drastically decreased after the KCN-treatment, while peaks at 173,183, 210, and 230 cm^{-1} remained relatively unchanged. The Cu/In ratio decreased to the 0.89–0.92 range after KCN-treatment. We therefore attribute the 260 cm^{-1} peak to the Cu–Se phase. On the other hand, the peak intensity of the 183 cm^{-1} shoulder decreased as *D* was decreased, whereas it remained unchanged after the KCN-treatment. González et al. [15] and Taguchi et al. [16] reported that the A_1 mode peak shifts to higher frequency as the pressure or compressive stress is increased. However, our results did not show these peak shift, but instead showed the peak at 183 cm^{-1} in addition to the A_1 mode at 173 cm^{-1}, suggesting that the peak at 183 cm^{-1} does not originate from compressive stress. On the other hand, Neumman [13] and Tanino [14] reported that there is an E mode peak around 180 cm^{-1}. To identify the peaks, we therefore did the polarization measurements of HH and HV configurations. (Fig. 7), and found that the relative intensity of the peaks at 210, and 230 cm^{-1} were different between these two configurations. This confirmed that these two peaks belong to non totally symmetric E or B_2 modes. On the other hand, the relative intensities of the peaks at 173, and 183 cm^{-1} were almost the

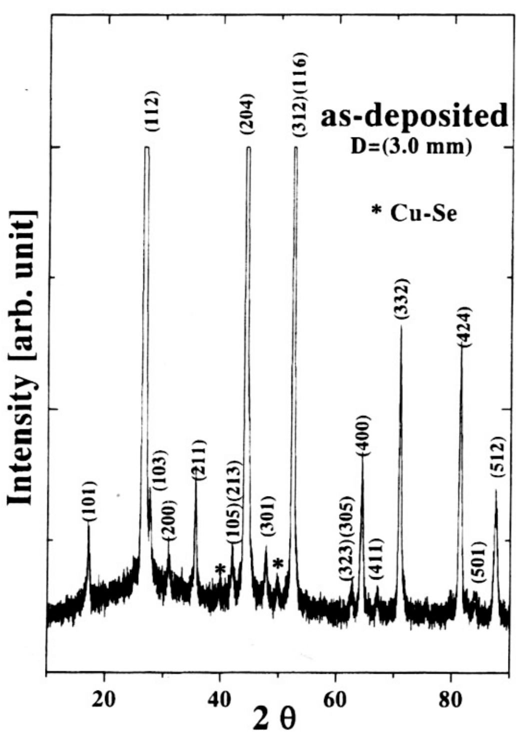

Fig. 4. XRD pattern of the as-deposited film.

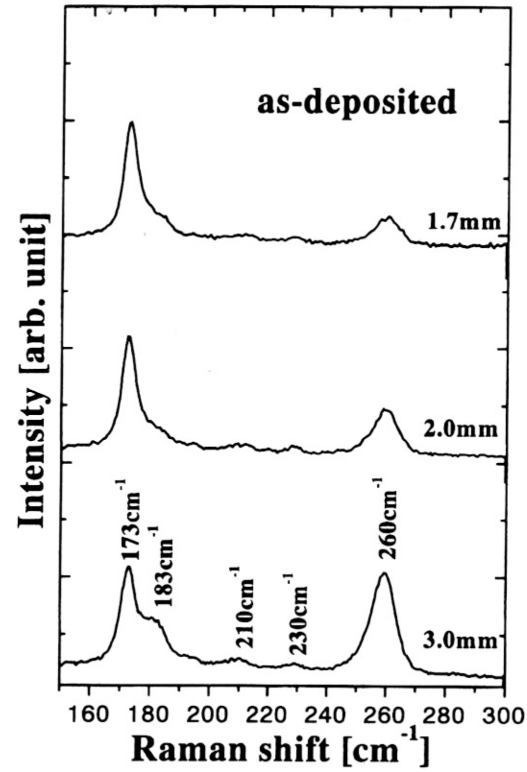

Fig. 5. Raman spectra of the as-deposited films.

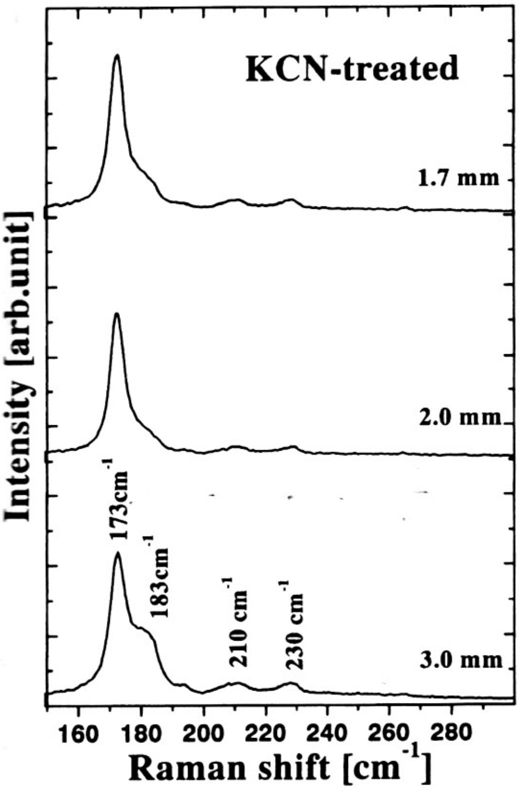

Fig. 6. Raman spectra of the KCN-treated films.

same for both the HH and HV configurations. These results suggest that the peak of 183 cm^{-1} is classified as totally symmetric mode. Fig. 8 shows the depth profile of Cu, In, and Se measured using SIMS for KCN-treated films of D = 3.0 and 2.0 mm. The Cu content for the D = 3.0 mm film was smaller than that for 2.0 mm and decreased near the surface region after the KCN treatment. Tuttle et al. [17] reported that when the substrate temperature is less than 400°C, the conversion process of Cu_xSe phase into $CuInSe_2$ is retarded due to limited Cu mobility, resulting in a very Cu poor surface layer ($CuIn_ySe_x$). However, we did not detect distinct XRD peaks of $CuIn_3Se_5$ nor In_2Se_3, suggesting that the origin of the 183 cm^{-1} Raman peak seems to be the localized Cu-poor $CuInSe_2$ phases that might show Raman mode with a symmetry similar to the A_1 mode of $CuInSe_2$. Yamanaka et al. [18] reported a similar phenomenon in their selenization process of Cu/In alloy, in which the peak intensity at 185 cm^{-1} decreased as the annealing temperature was decreased. Levoska et al. [19] also reported that in laser ablation the peak at 172 cm^{-1} became narrower with increasing substrate temperature. These results suggest that the 183 cm^{-1} Raman peak appear beside the A_1 mode of $CuInSe_2$ when the reaction temperature is not enough to grow stoichiometric $CuInSe_2$. These results also demonstrate that the nozzle diameter of the Cu crucible has an effect equivalent to those of temperature. Yamada et al. [12] reported that the energy of the cluster depends on the nozzle diameter and demonstrated that there is an optimum nozzle diameter. They showed that a crucible with a nozzle diameter larger than the critical size does not produces any high-energy clusters, because the pressure difference between the inside and outside of the crucibles is not very large. It is known that ionized clusters and neutral clusters enhance migration of adatoms and increase density of the nuclei [12]. The difference in nozzle diameter in the Cu crucible may affect the energy of the Cu cluster beam and therefore affect the crystal growth of $CuInSe_2$ by changes in the migration and nucleation. Our results show that the maximum nozzle diameter for obtaining good crystalline $CuInSe_2$ films was between 3.0 and 2.0 mm. The formation energy of Cu-Se compounds are lower than that of $CuInSe_2$ [18,20]. When the energy of the Cu cluster beam is low, as in the large nozzle diameter (D = 3.0 mm), the migration effect is negligible; therefore, reactions among Cu, In, and Se elements do not proceed rapidly, resulting in formation of Cu–Se binary phases at the surface and localized Cu-poor $CuInSe_2$ phase below the surface. The film of D = 3.0 mm showed the strong Raman peaks at 183 and 260 cm^{-1}. In

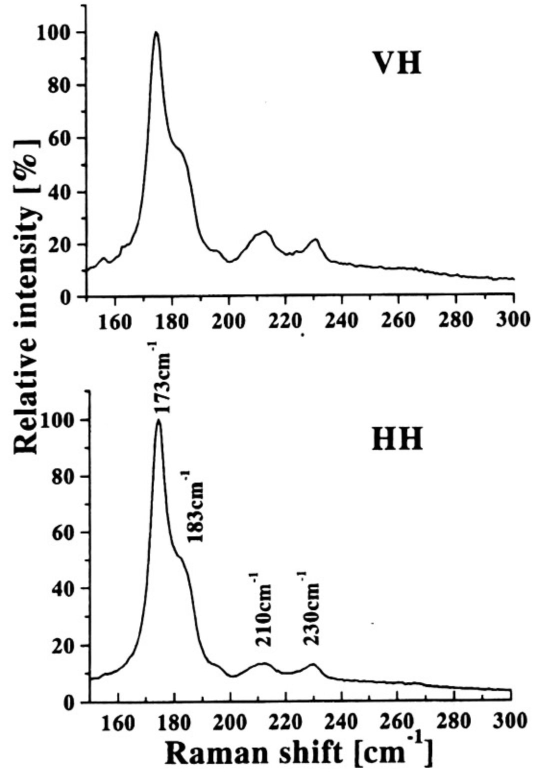

Fig. 7. Raman spectra of HH and HV configurations for the KCN-treated film deposited with D = 3.0 mm.

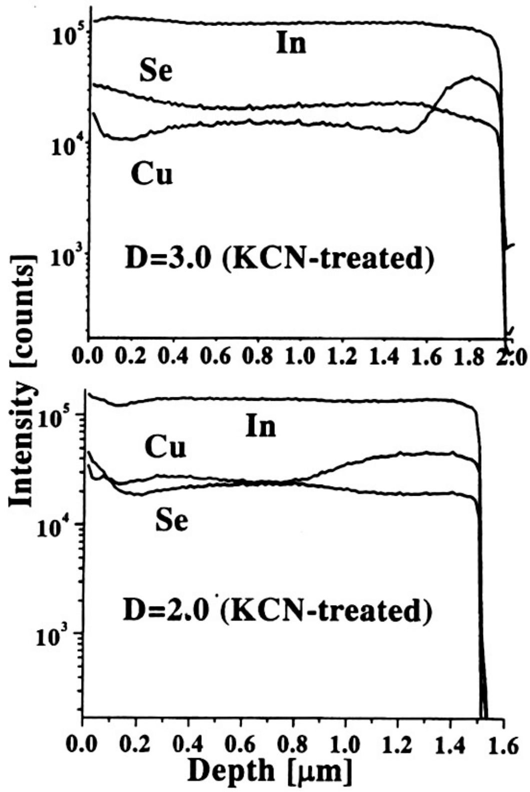

Fig. 8. SIMS depth profile of Cu,In and Se for the KCN-treated films deposited with $D = 3.0$ and 2.0 mm.

contrast to the energy level for $D = 3.0$ mm, when the energy of the Cu cluster beam was high (for $D = 2.0$ and 1.7 mm), most of the Cu, In, and Se reacted with each other, because of sufficient Cu cluster beam energy to form good crystalline $CuInSe_2$. This may be the reason why the Raman peaks at 183 and 260 cm^{-1} are weak in films prepared with a small nozzle diameter.

Our results show that the energy of Cu atoms plays a very important role in the formation process of $CuInSe_2$. These results also demonstrate that the nozzle diameter of the crucible can govern thin-film growth by affecting the energy of the cluster beam of individual elements, equivalent to the effect of substrate temperature.

4. Conclusion

$CuInSe_2$ films were grown by ICB and characterized by XRD, SEM, EPMA, SIMS, and Raman spectroscopy. The intensity of the Raman peaks at 183 and 260 cm^{-1} showed clear dependence on the nozzle diameter of the Cu source crucibles. The intensity of these two peaks decreased as the energy of the Cu cluster beam was increased. The grain size of the film and the Raman spectra showed that there is a critical nozzle diameter between 2.0 and 3.0 mm for obtaining good crystalline $CuInSe_2$ films. These results demonstrate that the energy of Cu atoms strongly affects crystal growth of $CuInSe_2$, and that the Raman peak at 183 cm^{-1} relates to localized Cu-poor $CuInSe_2$.

Acknowledgements

We thank S. Onari and K. Matsuishi of Tsukuba University for helpful discussions, H. Mori of Stanley R & D for taking SEM micrographs and EPMA measurements, and H. Toyotama for continuous support and encouragement.

References

[1] J.E. Jaffe, A. Zunger, Pys. Rev. B 29 (1984) 1882.
[2] D. Tarrant, R. Gay, J. Hummel, C. Jenson, Al. Ramos, Solar Cells 30 (1991) 549.
[3] K. Zweibel, H.S. Ullal, B.G. von Roedem, R. Noufi, T.J. Coutts, M.M. Al-Jassim, Proc. 23rd IEEE Photovoltaic Specialists Conf., 1993, p. 379.
[4] L. Stolt, J. Hedström, J. Kessler, M. Ruckh, K.O. Velthaus, H.W. Schock, Appl. Phys. Lett. 62 (1993) 597.
[5] B.M. Basol, V.K. Kapur, A. Halani, Proc. 22nd IEEE Photovoltaic Specialists Conf., 1991, p. 893.
[6] S. Matsuda, Y. Kudo, T. Ushiki, H. Inoue, K. Sato, Jpn. J. Appl. Phys. 31 (1992) 999.
[7] T. Ushiki, A. Ueno, T. Kai, H. Sano, H. Usui, K. Sato, Jpn. J. Appl. Phys. 32 (Suppl. 32–33) (1993) 103.
[8] H. Sano, S. Nakamura, K. Kondo, K. Sato, 1st World Conf. on Photovoltaic Energy Conversion, Waikoloa, 5–9 December 1994, pp. 179–181.
[9] H. Sano, K. Kondo, K. Sato, J. Cryst. Res. Tech. 31 (1) (1996) 349.
[10] K. Sato, Y. Yanase, T. Shimizu, T. Ishibashi, K. Kondo, Digest 9th Int. Photovoltaic Sci., Eng. Conf., Miyazaki, 12–15 November, 1996.
[11] Y. Yanase, K. Iida, Y. Kikuchi, T. Shimizu, T. Ishibashi, K. Sato, 9th Int. Photovoltaic Sci. Eng. Conf., Miyazaki, 12–15 November, 1996.
[12] I. Yamada, H. Takaoka, H. Inokawa, H. Usui, S.C. Cheng, T. Takagi, Proc. ISIAT'81 Int. Workshop on Ion-Based Technique, Tokyo, Kyoto, 1981, p. 449.
[13] H. Neumann, Solar Cells 16 (1986) 399.
[14] H. Tanino, T. Maeda, H. Fujikake, H. Nakanishi, S. Endo, T. Irie, Phys. Rev. B 45 (1992) 13323.
[15] J. Gonzáles, M. Quintero, C. Rincón, Phys. Rev. B 45 (1992) 7022.
[16] I. Taguchi, H. Ezumi, S. Keitoku, T. Tamaru, H. Osano, Jpn. J. Appl. Phys. 34 (1995) 135.
[17] J.R. Tuttle, M. Contreras, M.H. Bode, D. Niles, D.S. Albin, R. Matson, A.M. Gabor, A. Tennant, A. Duda, R. Noufi, J. Appl. Phys. 77 (1995) 153.
[18] S. Yamanaka, M. Tanda, N. Nakada, A. Yamada, M. Konagai, K. Takahashi, Jpn. J. Appl. Phys. 30 (1991) 442.
[19] J. Levoska, A.E. Hill, S. Leppävuori, O. Kusmartseva, R.D. Tomlinson, R.D. Pilkington, Jpn. J. Appl. Phys. 32 (Suppl. 32–33) (1993) 433.
[20] S. Zweigart, Th. Walter, Ch. Köble, S.M. Sun, U. Rühle., H.W. Schock, 1st World Conf. on Photovoltaic Energy Conversion, Waikoloa, 5–9 December, 1994, p. 60.